Article

Journal of
Nanoscience and Nanotechnology
Vol. 18, 5283–5291, 2018
www.aspbs.com/jnn

Copyright © 2018 American Scientific Publishers
All rights reserved
Printed in the United States of America

Field-Effect Transistor-Integration with TiO_2 Nanoparticles for Sensing of Cardiac Troponin I Biomarker

M. K. Md Arshad[1, 2, *], R. Adzhri[1], M. F. M. Fathil[1], Subash C. B. Gopinath[1, 3], and M. Nuzaihan M. N[1]

[1] *Institute of Nano Electronic Engineering (INEE),* [2] *School of Microelectronic Engineering (SoME),*
[3] *School of Bioprocess Engineering, Universiti Malaysia Perlis (UniMAP), 01000 Perlis, Malaysia*

The development of electrical biosensor towards device miniaturization in order to achieve better sensitivity with enhanced electrical signal has certain limitations especially complexity in fabrication process and costs. In this paper, an alternative technique with minor modification in the device structure is presented for signal amplification by implementing ambipolar conduction in the biosensor itself. We demonstrated the field-effect transistor (FET)-based biosensor coupled back-gate for attaining a higher sensitivity with the detection of lower target abundance. To utilize the coupled back-gate as a pre-amplifier, silicon-on-insulator wafer with thicknesses of top-silicon and buried oxide (BOX) layers of 70 nm and 145 nm, respectively were desired. Titanium dioxide (TiO_2) nanomaterial was deposited using sol–gel method on the channel which acts as a transducer. Surface functionalization on TiO_2 thin film allowed an effective immobilization of anti-cardiac troponin I antibody to interact cardiac troponin I (cTnI). Binding events at each step was validated by X-ray photoelectron spectroscopy (XPS) analysis. Further, electrical characterization (I_d–V_d) confirms the potentiality of FET-based biosensor to detect cTnI (represents acute myocardial infarction disease) with the concentration ranges from 10 μg/ml down to 1 fg/ml. The sensitivity of 459.2 nA $\cdot$ (g/ml)$^{-1}$ and lower detection limit of 1 fg/ml were achieved at $V_{bg} = -5$ V and $V_d = 5$ V. The designed device demonstrates its ability to detect lower level of cTnI with pre-amplified electrical signal by back-gate biasing.

Delivered by Publishing Technology to: [illegible]
IP: [illegible] On: Mon, 19 Mar 2018 13:34:28
Copyright: American Scientific Publishers

Keywords: Biosensor, Bioelectronic, Electrical-Based, Field-Effect Transistor, Titanium Dioxide Thin Film, Back-Gate Coupling, Cardiac Troponin I.

1. INTRODUCTION

Effective, simple, and accurate are essentials in disease diagnosis for the subsequent adequate and appropriate treatment. One of the reasons for death is the delay in diagnosis due to time-consuming process, which causes the disease to rapidly evolve and devour the host. Therefore, studies on the application of biosensor with high sensitivity and instantaneous detection have attracted considerably among researchers.[1] At present, the conventional biomarker techniques (e.g., western-blot, dot-blot, gel-shift, and enzyme-linked immunosorbent assay (ELISA)) are depending on qualitative display and laborious.[2] These techniques require the usage of 'labels' or 'tags' to detect a particular analyte from other background materials. They are still considered to be lacking in sensitivity, specificity, highly expensive, and can only be conducted within the laboratory setup. The adaptation of biosensor towards electrical-based characterization has opened a new avenue for label-free approaches.[3] Additionally, it also elevates several features with fast detection, low-cost, high sensitivity, and excellent specificity. Several types of electrical-based biosensor have established its reputation with their own specialty such as integration of nanowire (NW),[4] interdigitated electrode (IDE),[5] screen printed electrode (SPE),[6] and field-effect transistor (FET).[7, 8] These devices prove their capabilities and potential to become a primary choice for biomolecular detection in the near future.

*Author to whom correspondence should be addressed.

The versatility of FET device for electronic switching has been well-recognized through a vast development of electronic products with diverse functionalities and portability.[9–11] For biosensing applications, the FET-based biosensor is a choice with special characteristics such as,

(1) ability to directly translate the interaction of probe-analyte on the FET surface into a readable signal;
(2) higher sensitivity, thus lower concentration of target detection can be achieved;
(3) compatible with silicon CMOS fabrication processes, thus integration with silicon technologies is not an issue, in fact it is the main advantage. The FET-based biosensor can be divided into four main structures i.e., source, drain, channel, and back-gate electrodes (for device with back-gate electrode).

The source, drain, and back-gate are for electrical interconnection, while the channel is transducing area, converts external charge of biomolecular interaction to the main electrical biasing of the device. Recent developments on FET-based biosensors show a promising result with excellent specificity, sensitivity, and possess the ability to detect ultra-low concentration of the target biomolecule.[12] Unfortunately, the approach with handheld portable device is still beyond from possible as the output signal or current is considered low and can only be read by high performance non-portable electrical readers.[13] The development of the back-gated FET biosensors is to attempt on the signal amplification technique with the ambipolar conduction (either holes or electrons in the channel occurs depending on the secondary gate biasing) to overcome the current issues.[14]

IP: 185.14.195.115 On: Tue
Copyright: American Scientific Publishers
Delivered by Ingenta

For a transducer material, titanium dioxide (TiO_2) can be utilized as energy transducing nanomaterial,[15] has several advantageous such as excellent electrical properties, physical durability, and strong chemical interaction.[10, 16, 17] Additionally, the availability of oxygen group within the TiO_2 nanomaterial is useful for functionalization processes. The functionalized surface allows/enables interaction between the charged biomolecule and the FET transducer channel, thus, detection procedure can be accomplished. The integration of TiO_2 nanomaterial with FET devices is essential to tailor the functionalized surface for detection purposes. TiO_2 nanomaterial can be deposited with thin film structural design by using different methods, e.g., sputtering,[18] chemical vapor deposition (CVD),[19] and sol–gel technique.

To demonstrate the biosensing ability of the designed FET-coupled back-gate, acute myocardial infarction (AMI), a myocardial cell death due to prolonged myocardial ischemia, leads to mortality was taken as a model system. With AMI diseases, minor symptom initiate when coronary artery carries oxygenated blood along the cardiac muscle that has been obstructed with fat. As a result, the cardiac muscle slowly damages due to the oxygenated blood could not be circulated within the organ itself until it reaches AMI level. At the same time, a protein-based molecule called cardiac troponin I (cTnI) secretes from the damaged cardiac muscle. cTnI (cardiac antigen) is an ideal and gold standard biomarker for AMI detection due to its longevity and responsiveness when interact with its complementary antibody. The concentration level of cTnI can be correlated to the severity of AMI.[20] Early detection are really beneficial for early treatment, changing the life style, and preventing irreversible damage to the heart.[21] Currently, electrocardiogram (ECG) is the recommended test for AMI, but it relatively lacks sensitivity, especially in patient with unstable angina and non-ST segment elevation myocardial infarction (NSTEMI). Moreover, ECG needs to be performed at the 'right' moment to capture the abnormal signal and cannot be considered as early detection. To complement that, cTnI has been widely used for diagnosis of AMI and it offers higher sensitivity, specificity, and remain elevated in the blood for longer period than any other cardiac biomarkers. Standard assays to detect cTnI biomarker, such as ELISA, fluorescence,[22] electrochemiluminescence immunoassay,[23] and surface plasmon resonance (SPR).[24] These techniques employ highly sophisticated separative procedures that involve high cost. Since they are performed in central laboratories of clinics and hospitals, suffering from time-consuming process, which often requires high skilled laboratory personal as well as significant investment of resources into procuring specialized equipment. Therefore, they are highly incompatible with the quick decisions for early detection and cannot be performed as point-of-care (POC) testing.

Diagnostics with POC have been attracted with more interest since they provide a fast result especially at emergency department, but it shouldn't forgo the accuracy result. Although some commercial test kits are available (based on either fluorescence or ELISA) to provide POC, detection with these kits usually provide only qualitative results and relatively expensive.[25] The accuracy of detection provided by POC is still bringing debatable among the society as is not equal to that of a good lab test,[26] thus existing commercial POC tests are not used as main diagnostic element or even can't be used as decision making tool.

In this work, we utilized the concept of FET coupled back-gate in diagnostic to find the elevated cardiac troponin level in the bloodstream. The FET-based biosensor with back-gate biasing, fabricated on silicon-on-insulator (SOI), allows the modulation of the conductivity from the bottom to the semiconductor channel. Secondly, in term of fabrication, it has less challenges and difficulties compared to 1D nanowire materials. We expect the current study offers a label-free detection with higher sensitivity than label-based approach, in addition to address the unmet demand of a system for accurate, high sensitivity, and fast diagnosis of the cardiac biomarker level.

2. EXPERIMENTAL DETAILS

2.1. Fabrication of Back-Gated FET-Based Biosensor

Industrial grade SOI wafer (SOITEC, France) was used to fabricate the device with top-down photolithography method. The SOI structure comprises of three layers i.e., bottom silicon (Si) substrate, buried oxide (BOX), and top Si layers with thicknesses of ~1000 μm, 145 nm, and 70 nm, respectively. The fabrication of back-gated FET biosensor is initiated by cleaning the SOI wafer by using piranha solution [H_2SO_4 (3): H_2O_2 (1)] for organic contaminant removal, RCA 1 [H_2O (5): NH_4OH (4): H_2O_2 (1)] for metallic contaminant, buffered oxide etch (BOE) for native silicon dioxide (SiO_2) removal and rinsed with deionized (DI) water. Next, photolithography process is started by coating a thin layer of RD6 photoresist (PR) using spin coater with 3000 rpm rotation for 30 s and soft-baked on a hot plate at 100 °C for 90 s. Afterward, the device is subjected to UV exposure process for 10 s with first mask to form source and drain regions, then straight to second soft-bake process in advance of PR developing process. The device then is dipped into RD6 photoresist developer solution for ~15 s until the UV exposed PR is removed completely. Missing hard bake process of photoresist after development process. Usually around 120 minutes at 100/110 degree celcius. Subsequently, the device is exposed to the reactive ion etching (RIE) (ICP-RIE 101, Samco, Japan) plasma for the purpose of Si removal on the micrometer-gap connecting between source and drain, as well as the back-gate electrode area. The exposed Si is bombarded with CF_4/O_2 plasma with ICP-RIE standard recipe of tetrafluoromethane (CF_4) at 25 sccm and oxygen (O_2) at 3:1 sccm. The Inductive Coupled Plasma (ICP) power is set at 100 W and the chamber pressure is set to 100 mTorr. Next, similar photolithography process with secondary mask is conducted for back-gate region. The PR is developed, merely expose the back-gate region. The top-Si is etched with RIE method with same parameter as in previous process, exposing the BOX layer. Subsequently, BOX layer is etched by using BOE solution, the device is dipped into BOE for ~30 s revealing the substrate Si. Next the TiO_2 thin film is deposited on top of the device, covering the entire surface. Then, the device is coated with thin layer of aluminum (Al) by using thermal evaporator process. Al is used as a sacrificial layer to allow TiO_2 removal by using RIE. After patterning the TiO_2 thin film, completion stage of device is attained after deposition of another Al thin film and the metal contact are formed at source, drain, and back-gate region by final photolithography process with Al etches to remove the unwanted Al thin film. The completed device is illustrated in Figure 1.

2.2. TiO_2 Thin Film Deposition

TiO_2 thin film is synthesized by using sol–gel method. The preparation of sol–gel is a combination of three types of chemical solutions i.e., Titanium (IV) isopropoxide [$Ti(OCH(CH_3)_2)_4$] (TTIP), ethanol, and acetic acid that act as a precursor, solvent, and stabilizer, respectively, with a

Copyright: American Scientific Publishers
Delivered by Ingenta

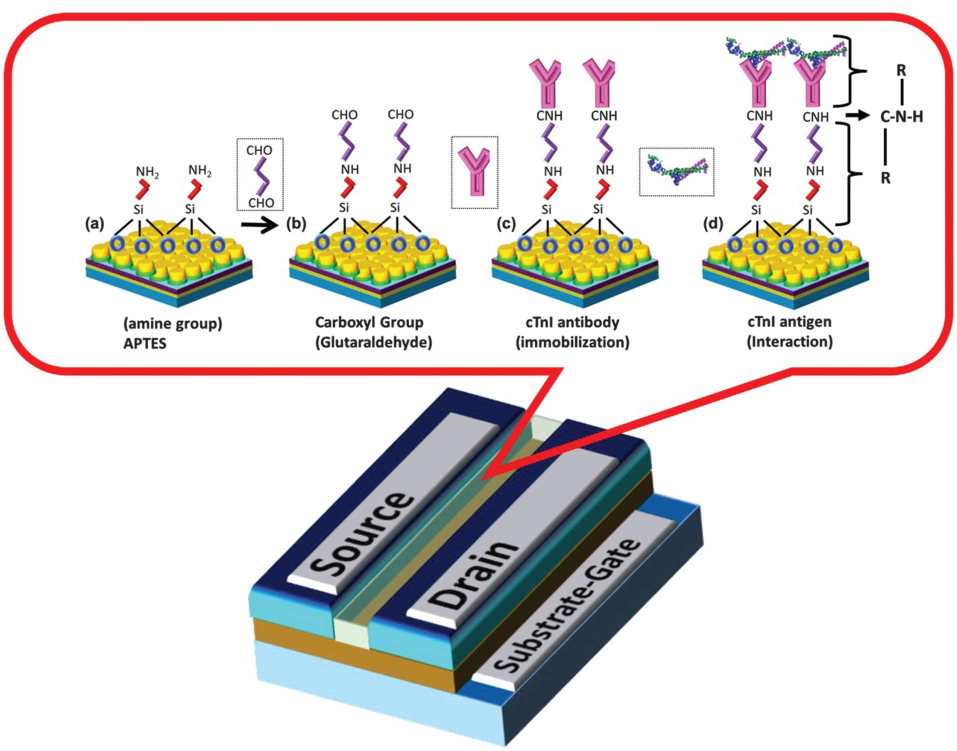

Figure 1. Surface functionalization process involving covalent binding of (a) APTES, (b) GA, (c) cTnI antibody immobilization, and (d) cTnI antibody-antigen interaction.

ratio of (1:9:0.1). At first, ethanol is poured into a beaker and heated at 90 °C using the hot plate. Simultaneously, ethanol is stirred by using magnetic stirrer with spin speed of 600 rpm for 15 minutes. Then, TTIP is dropped and mixed with the ethanol, changing the solution from colorless into cloudy solution. The stirring process is continued for an hour. Next, acetic acid is dropped until the solution turns crystal clear. The solution is continued to be heated and stirred for another three hours with the same temperature and speed. After the process ended, the sol–gel undergo aging process for 24 hours to stabilize the solution, preventing TiO_2 thin film from cracking at the deposition process stage. For TiO_2 thin film deposition, the device is placed inside the spin coater and placed on a vacuum stage to hold the device while spin coating process is conducted. The TiO_2 sol–gel is coated completely on top of the device and spun at 3000 rpm for 30 s. Then, the TiO_2 coated device is baked at 100 °C for 10 minutes. The achieved thickness for one layer deposition of TiO_2 by spin coating method is ∼100 nm.[27] In this work, the spin coating process is repeated three times, thus increasing the thickness of TiO_2 thin film up to 300 nm. Next, the thin film is annealed at 550 °C inside the muffle furnace (Nanjing Oxy Tech., Oxy2-4-Lot, China) for one hour. The purpose of annealing process is to change the crystallinity into anatase type,[27,28] reduce particle dislocation,[29] and enhance the electrical conductivity.[30] Finally, the Al thin film is deposited, patterned for the purpose of TiO_2 etching mask. The etching is conducted by using RIE method with previous reported recipe.[31,32] In addition, another TiO_2 thin film is fabricated on top of 1×1 cm silicon dioxide (SiO_2) wafer, specifically made for X-ray photoelectron spectroscopy (XPS) characterization.

2.3. Surface Functionalization

Due to the oxygen (O) functional group of TiO_2, the device can be functionalized to gain the ability to detect cTnI antigen. To functionalize, first the TiO_2 thin film surface is treated by immersing the device into ethanol solution, promoting the number of free hydroxyl (OH) functional group. Next, 2 μl of 2% (v/v) 3-Aminopropyltriethoxysilane (APTES) solution is dropped on the OH-terminated TiO_2 thin film to promote amine group (NH_2) as illustrated in Figure 1(a). Subsequently, 2 μl of 2.5% (v/v) glutaraldehyde (GA) solution is dropped on NH_2 bonded TiO_2 thin film. The end-to-end aldehyde group structure of GA will experience chemical reaction, thus promoting aldehyde group with another end bonded with the NH_2 group as depicted in Figure 1(b). 10 μg/ml of cTnI antibody is dropped, the immobilization between the cTnI antibody-GA occurred due to the amine group of antibodies befits with the aldehyde group, creating a strong covalent bonding between those two functional groups (Fig. 1(c)). As a final point, the cTnI antigen

IP: 185.14.195.115 On: Tue, 20 Mar 2018 10:34:28
Copyright: American Scientific Publishers

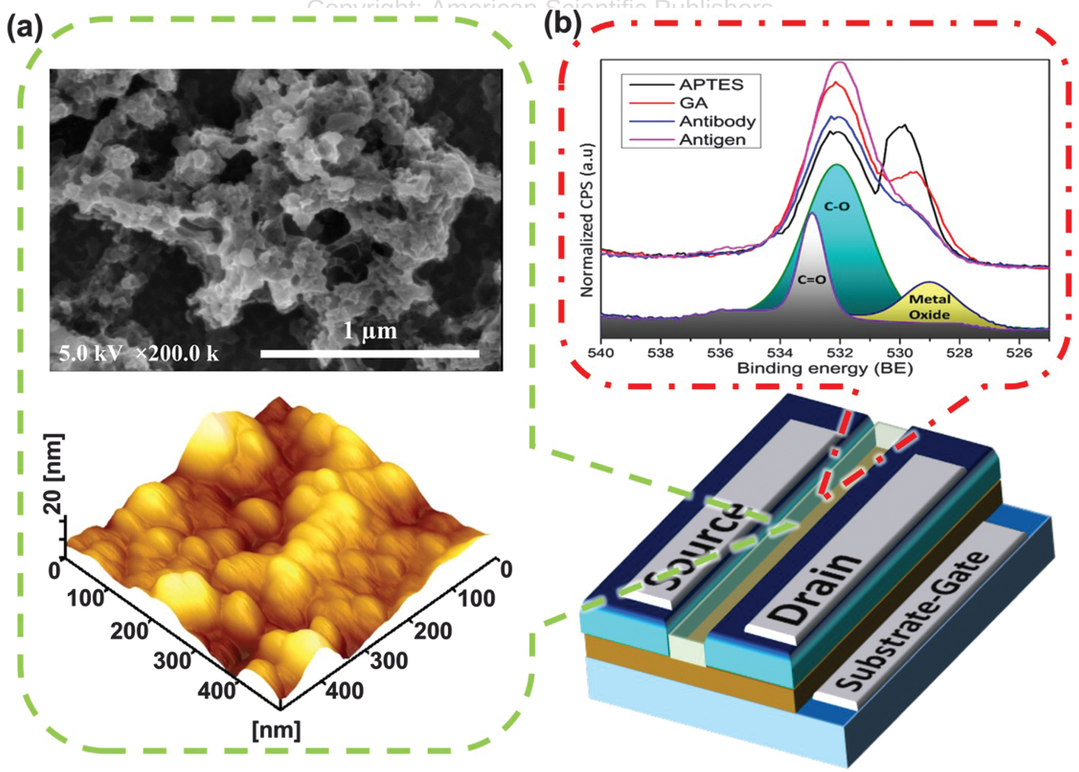

Figure 2. Various characterizations of TiO_2 thin film nanoparticles including (a) surface morphological by using FESEM and AFM, as well as (b) normalized XPS peak profile for each surface functionalization processes with three types of quantified O bonding peak.

with various concentrations from 1 fg/ml until 10 μg/ml are allowed to be bonded naturally to permit antibody-antigen interaction (Fig. 1(d)). To determine the specificity of the device, two types of negative control sample (PBS buffer (pH 7.4) and 10 μg/ml of cTnT) are dropped (2 μl) prior to the cTnI antigen detection. Additionally, as for maximizing the reaction between each surface functionalization, incubation process inside the dry cabinet is performed for two hours.

2.4. Characterization of TiO_2 as Transducing Material

To confirm the existence of deposited nanomaterial, two types of characterization are carried out i.e., physical and electrical characterizations. Initially, physical characterization is conducted by using high power microscope (HPM) (OLYMPUS-BX51, Japan) to determine the structural design of fabricated devices. Next, field emission scanning electron microscopy (FESEM) (FEI, NovaNanoSEM, USA) and atomic for microscopy (AFM) (SPA400, Seiko instrument inc. Japan) are utilized to characterize the nanoscopic structure of TiO_2 thin film. Then, XPS (Omicron nanotechnology, Germany) is used to validate the functional group binding of each surface functionalization. Subsequently, electrical characterization is carried out to examine the conductivity and sensitivity of the TiO_2 FET-based biosensor by using surface parametric analyzer (Keithley 6487 picoammeter, USA).

3. RESULTS AND DISCUSSION

3.1. Unique Back-Gated FET-Based Biosensor with Pre-Amplifier

FET-based sensor with an electronic switching has been well attested with a wide range of achievements having versatile functionalities and portability. Past developments on FET-based biosensors display a concrete result with higher specificity and sensitivity.[12] However, the current approaches with handheld device is still having hurdles due to very low current generated and only be transduced by high performance laboratory-equipped electrical readers.[13] This issue has the possibility to overcome by developing back-gated FET biosensor to amplify the signal using ambipolar conduction.[14, 33] In the present work, we availed a substitute technique by tuning the device structure for signal amplification by ambipolar conduction. This concept

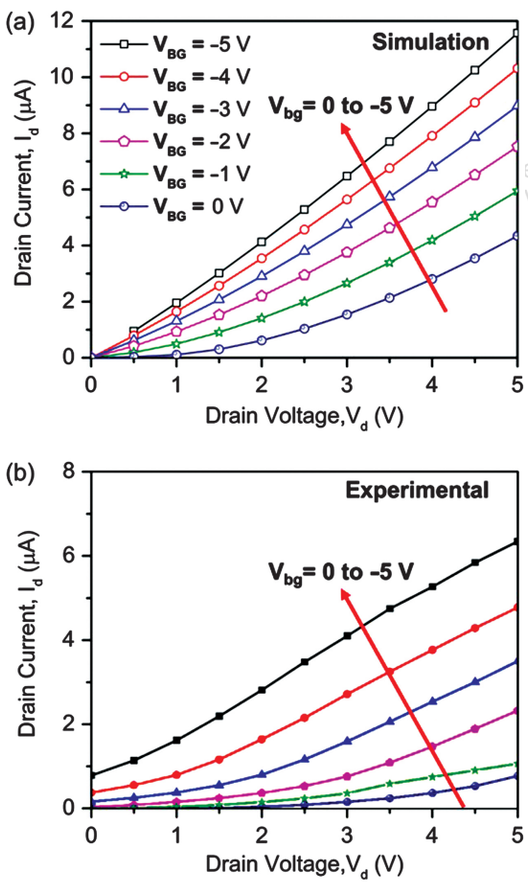

Figure 3. I_d–V_d characteristics comparison between (a) simulation and (b) experimental of FET-based biosensors of bare device with the presence of TiO_2 as transducer and back-gated biasing. V_d is sweep from 0 V to −5 V and various V_{bg} biasing (from 0 V to −5 V).

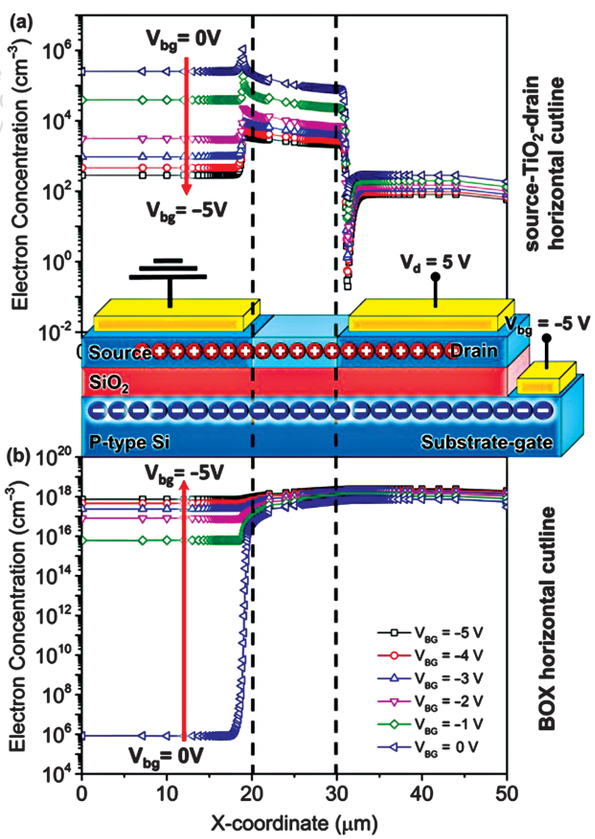

Figure 4. Graphical representation of electron concentration with V_d = 5 V and various V_{bg} biasing (from 0 V until 5 V) along (a) source-TiO_2-drain and (b) BOX/substrate layer.

with FET-coupled back-gate is to diagnose abnormal cardiac troponin lower level in the patient blood sample.

3.2. Physical Characterization of TiO_2 Thin Film and Surface Modification Bonding Analysis

The deposited TiO_2 thin film was observed within nanoscopic level to determine the grain boundary, which is crucial to acquire excellent electrical characteristic.[34] The formation of grain boundary of TiO_2 thin film is clearly seen from AFM and FESEM images (Fig. 2(a)). AFM scan area size is 1×1 μm and FESEM magnification is 200,000×. Both images (AFM and FESEM) show a similar characteristic of grain boundary with average grain size of 200 nm. Additionally, AFM results show that the TiO_2 thin film possess an average roughness (R_a) of ~1.4 nm. Low roughness of TiO_2 thin film within nanosize particle scale allows excellent electrical distribution along the devices. Afterward, XPS was used to determine the element or chemical bonding on a surface of functionalized TiO_2 thin film. Each surface functionalization processes i.e., APTES, GA, cTnI antibody, and cTnI antigen were scanned to confirm the existence of desired functional group as presented in Figure 2(b). The scanning image is mainly focus on the carbon (C) and oxygen (O) element spectrums. It reveals two of functional groups i.e., C═O, C–O, and metal oxides (TiO_2). The characterization of the first linker (APTES) revealed all of the functional group i.e., C–O and C═O and metal oxide. Based on the structure, APTES does not contain any C and O bonding. The presence of C–O and C═O almost certainly from the C defected metal oxides as the metal oxide possess the highest count.[35] Afterward, secondary linker (GA) increases the amount of C–O and C═O as the GA structure contain the aldehyde (H–C═O) and (C–C) group. In the opposite, metal oxide peak becomes less as the TiO_2 thin film is away from the scanning range. Subsequently, immobilization of cTnI antibody reduces the peak of C–O and C═O, ranked into the third highest as compared to the reaction between amine group (APTES) and the aldehyde (GA). The bonding formed a new functional group i.e., R–C–N–H–R (Fig. 1(d)), where R is another large chain of chemical structure at both end. Next, cTnI antigen-antibody interaction produces the highest peak of C–O and C═O. The formation of C and O bonding is due to the multi-types

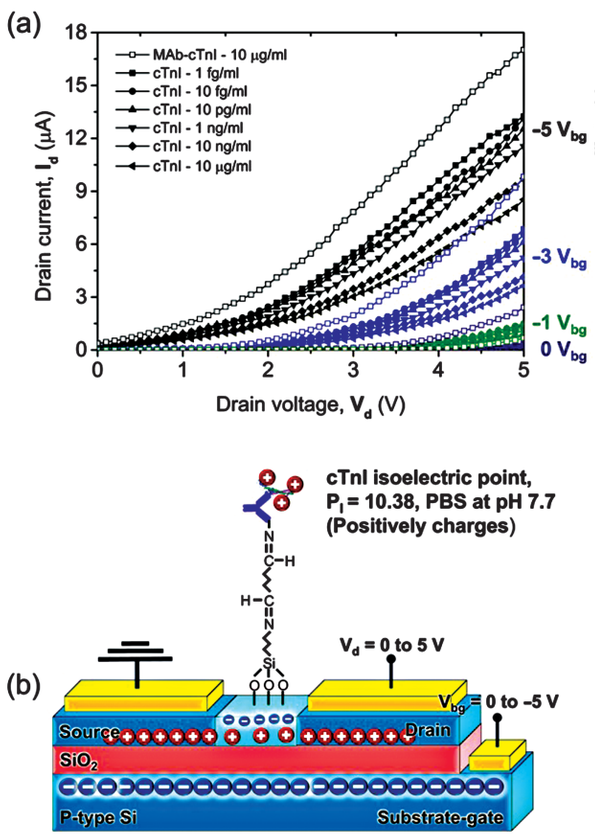

Figure 5. Different concentration of cTnI biomarker detection by using FET-based biosensor. (a) I_d–V_{bg} characteristics by sweeping V_d from 0 V to 5 V at voltage step of 0.1 V and various V_{bg} biasing (from 0 V to −5 V). (b) Charge interaction between the device and cTnI antigen.

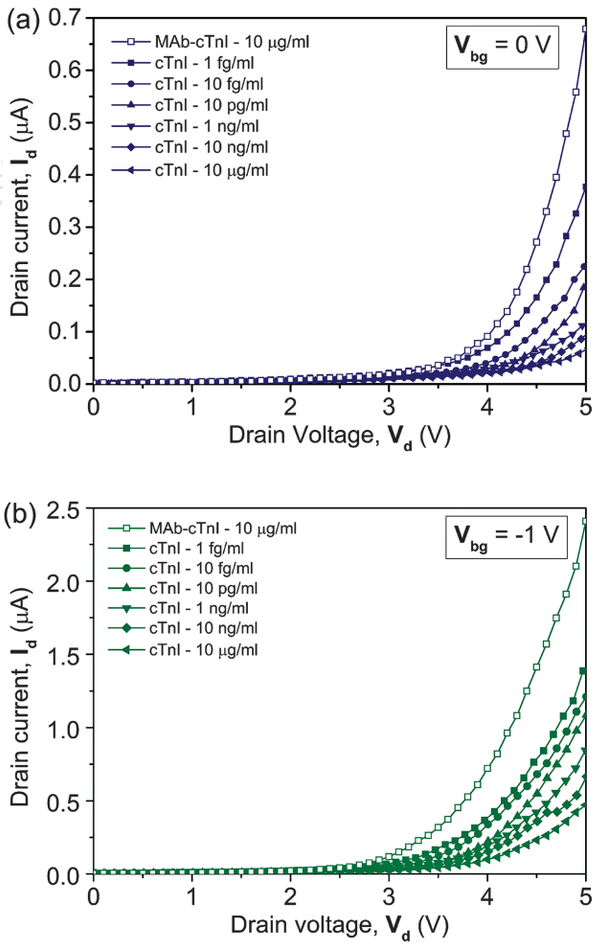

Figure 6. Split electrical result of the detection of cTnI antigen with different back-gate biasing of (a) 0 V and (b) −1 V.

of binding that exist within the large amino acid chemical structure in the cTnI antigen. From the XPS result, it has been confirmed that TiO_2 thin film structure can uphold the covalent bonding. TiO_2 surface can be modified without jeopardizing the inner molecular structure that can disrupt the electrical characteristic, which is crucial to maintain the stability and sensitivity of the device.

3.3. Electrical Characterization of Bare TiO_2 FET-Based Biosensor

To confirm the capability of the back-gate to amplify the electrical conductivity flow through the transducer material (TiO_2) and further used to modulate the antigen-antibody interaction signal, the effect of back-gate biasing on the bare devices (non-functionalized TiO_2 thin film) is demonstrated. The device is supplied with two types of voltage supplies i.e., drain voltage (V_d) and back-gate voltage (V_{bg}) as an input. Figure 3 shows (a) simulation and (b) experimental for the I_d–V_d as a function of V_{bg}. Both simulation and experiment were conducted with the same electrical parameters i.e., V_d sweep from 0 V to 5 V and V_{bg} from 0 V to −5. Further, it can be seen that both simulation and experimental, although it is not identical, it exhibits similar trend, thus justified to be used for further analysis.

The I_d–V_d increases as a function V_{bg}, can be explained with the following, the substrate/BOX interface rich of electron when V_{bg} supplied with negative bias, thus accumulation of hole occurs at the TiO_2/BOX interface (Fig. 4(a)), which in turn enhance the holes' buildup at the source-TiO_2-drain interface increasing the electrical conductivity as illustrated in Figure 4(b). The result proves that the device attains its functionality to amplify the electrical signal by V_{bg} modulation and TiO_2 shows a potential biosensor platform with excellent electrical responsiveness and exhibit outstanding electron-transfer kinetics.

3.4. Electrical Characterization of cTnI Protein Detection

As previously explained in XPS characterization, the cTnI antibody was successfully immobilized on the TiO_2 thin

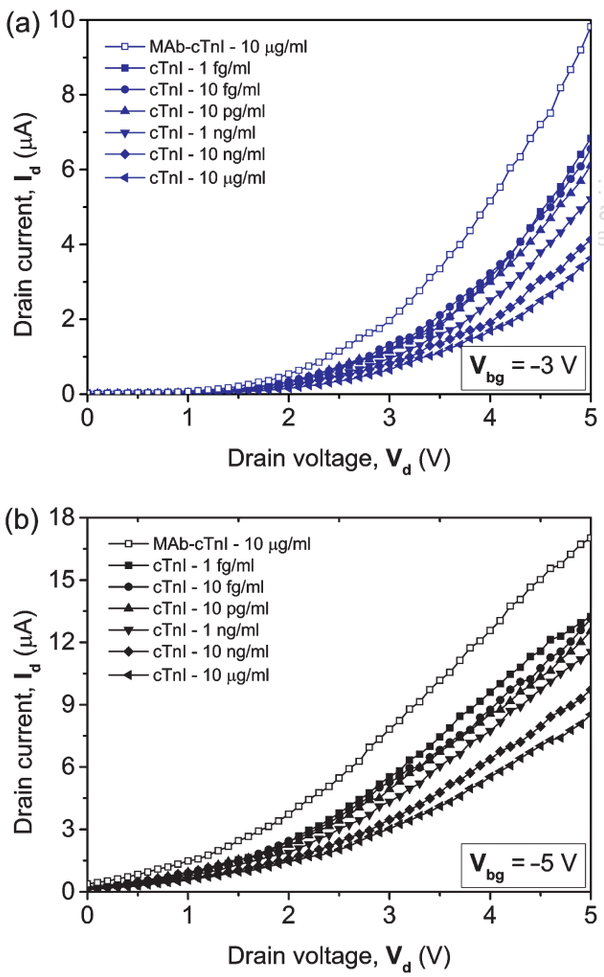

Figure 7. Split electrical result of the detection of cTnI antigen with different back-gate biasing of (a) −3 V and (b) −5 V.

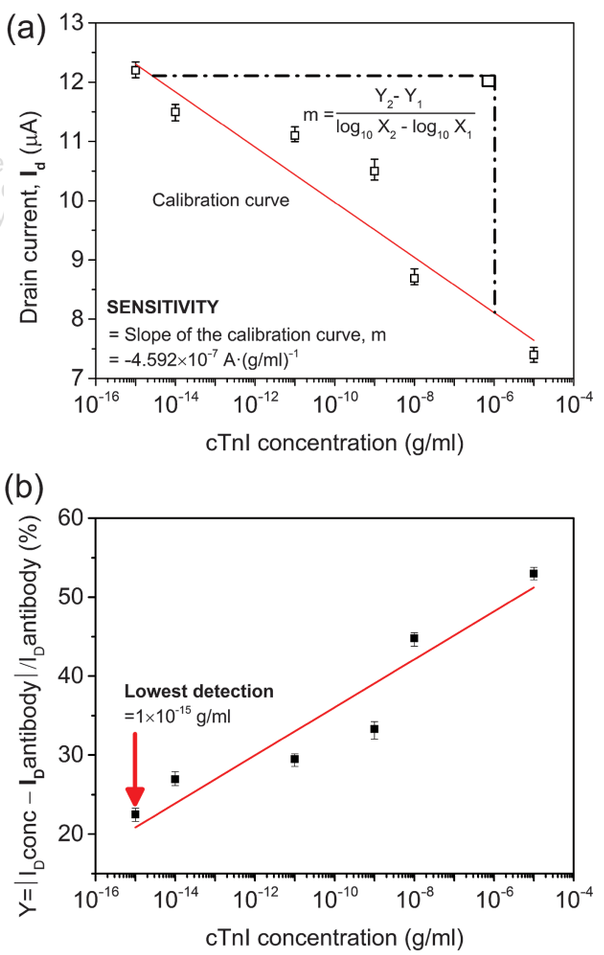

Figure 8. The performance of FET-based biosensor for cTnI detection based on its (a) sensitivity and (b) LOD.

Table I. Comparison on various devices and techniques of cTnI detection based on dynamic detection range and LOD.

Device type	Linear range (g/ml)	LOD (g/ml)	Reference
Gold nanoparticles modified carbon electrode	1.6×10^{-11}–1.6×10^{-9}	3.4×10^{-12}	[39]
CMOS-compatible, label-free silicon-nanowire	9.2×10^{-11}–4.6×10^{-8}	9.2×10^{-11}	[40]
G-aminobenzoic acid film-based immunoelectrode	5.0×10^{-11}–5.0×10^{-9}	1.6×10^{-11}	[41]
Carbon nanofiber-based nanoelectrode arrays	2.0×10^{-10}–1.0×10^{-7}	2.0×10^{-10}	[42]
Fluorescent immunosensor via spatially-controlled polymeric	2.0×10^{-12}–1.0×10^{-10}	2.0×10^{-12}	[43]
Rapid electrical immunoassay through dielectrophoretic concentration using imbedded electrodes	1.0×10^{-12}–1.0×10^{-7}	7.0×10^{-13}	[44]
TiO_2 integrated back-gate coupling FET-based biosensors	1.0×10^{-15}–1.0×10^{-5}	1.0×10^{-15}	This work

film. To determine the ability of the back-gate biasing towards the amplification of electrical signal of cTnI antibody and antigen, V_{bg} is biased at 0 V, −1 V, −3 V and 5 V with V_d constant sweep from 0 V until 5 V. The detection was conducted starting from the lowest cTnI antigen concentration (1 fg/ml) and continuously increase until 10 μg/ml. As illustrated in Figure 5(a), the graph shows that the current decreases as the cTnI concentration is increased with Figures 6 and 7 represents the split result for different back-gate biasing.

The decrease in current is related to decrease in conductance, similarly as previously reported.[36, 37] This is due to highly related *p*-type TiO_2 thin film characteristic and the augmentation from the positively charged biomolecules ($P_I = 10.38$, PBS = pH 7.4), resulting the highest current level produces by $V_{bg} = -5$ V. TiO_2 modified FET biosensor is *p*-type material as the TiO_2 thin film possess higher oxygen over the titanium composition.[38] Thus, with combination of negative V_{bg} and *p*-type TiO_2, accumulation of holes occurs in the TiO_2 channel. However, with additional positive charges (from the cTnI antigen), it creates a weak inversion layer (electron) accumulated at channel as illustrated in Figure 5(b), thus the current signal is signified. To ensure the quality of the detection, negative target is then added prior to evaluate the cTnI antibody-antigen interaction. PBS buffer and cTnT antigen are tested onto the antibody probed TiO_2 thin film.

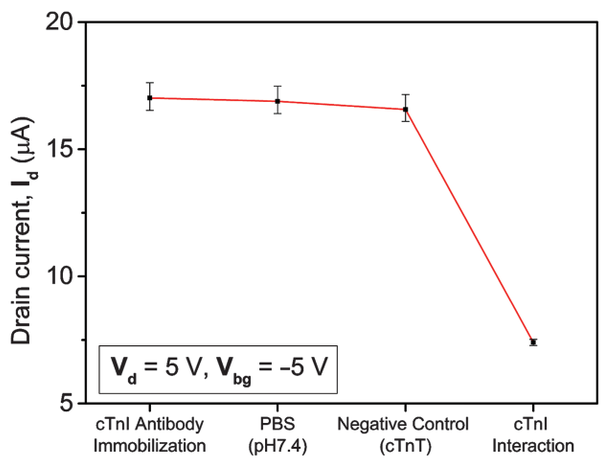

Figure 9. Electrical result for device specificity with two negative control (i.e., PBS and cTnT antigen (10 μg/ml)) and cTnI target protein (10 μg/ml).

Further analysis was conducted to determine device sensitivity and limit of detection (LOD), related to I_d value and cTnI antigen concentration. Sensitivity of the device can be defined by the slope calibration curve (Fig. 8(a)) which is directly related to the *I*–*V* characteristics of cTnI detection (Fig. 5(a)). The sensitivity attained from the plotted graph is 459.2 nA · (g/ml)$^{-1}$, taken at the highest current i.e., $V_{bg} = -5$ V and $V_d = 5$ V. Next, the LOD has been taken into consideration. The antibody current value was used as references to calculate the percentage of difference between cTnI antigen and cTnI antibody current flow, then plotted against cTnI concentrations (Fig. 8(b)). The experimental result shows that the device was able to detect ultra-low cTnI antigen concentration (1 fg/ml) with high stability.

IP: 188.14.195.116 On: Tue, 27 Mar 2018 10:34:28
Copyright: American Scientific Publishers
Delivered by Ingenta

A comparison among the lowest detections has been made with previously reported studies (Table I), showing that this device proved to have the lowest LOD, the widest range of detection and has the ability to amplify the electrical signal with excellent sensitivity.

To finalize the investigation, Figure 9 shows that PBS buffer and cTnT antigen display negligible changes, compared to the non-interact cTnI antibody condition. This result contradicts to cTnI antigen, which showed remarkable changes to reflect the device capability to detect specific biomolecules.

4. CONCLUSION

We have demonstrated the effect of back-gate biasing with the purpose of enhancing the electrical conductivity of FET-based biosensors. A transducer material (TiO_2 thin film) was deposited using sol–gel method on the channel between the regions of source and drain. For surface chemical functionalization, the process was initiated with deploying two types of linker (APTES and GA) followed by the immobilization of cTnI antibody. The results showed that the FET-based biosensors coupled back-gate has potential to amplify the electrical signal, which can be correlated with simulation results. For the detection of cTnI, a great pre-amplification signal was demonstrated. The sensitivity of 459.2 nA · (g/ml)$^{-1}$ and LOD with 1 fg/ml of cTnI can be achieved at negative

V_{bg} and positive V_d with *p*-type TiO_2 material. This study offers a label-free detection in high performance manner and addresses the current unmet demand of fast diagnose the low abundant cardiac biomarker.

Acknowledgments: The authors are grateful to the Department of Higher Education, Ministry of Higher Education, (KPT) for funding this research through the Fundamental Research Grant Scheme (FRGS) with the grant number 9003-00536. The author also would like to acknowledge all the team members in Institute of Nano Electronic Engineering (INEE), Universiti Malaysia Perlis (UniMAP) for their guidance and help.

References and Notes

1. S. Cheng, K. Hotani, S. Hideshima, S. Kuroiwa, T. Nakanishi, M. Hashimoto, Y. Mori, and T. Osaka, *Materials (Basel)* 7, 2490 (**2014**).
2. G. Zhang and Y. Ning, *Anal. Chim. Acta* 749, 1 (**2012**).
3. S. Liu and X. Guo, *NPG Asia Mater.* 4, e23 (**2012**).
4. M. N. M. Nuzaihan, U. Hashim, M. K. Md Arshad, S. R. Kasjoo, S. F. A. Rahman, A. R. Ruslinda, M. F. M. Fathil, R. Adzhri, and M. M. Shahimin, *Biosens. Bioelectron.* 83, 106 (**2016**).
5. S. K. Tuteja, M. Kukkar, C. R. Suri, A. K. Paul, and A. Deep, *Biosens. Bioelectron.* 66, 129 (**2015**).
6. P. Sharma, S. K. Tuteja, V. Bhalla, G. Shekhawat, V. P. Dravid, and C. R. Suri, *Biosens. Bioelectron.* 39, 99 (**2013**).
7. R. Adzhri, M. K. Md Arshad, S. C. B. Gopinath, A. R. Ruslinda, M. F. M. Fathil, R. M. Ayub, M. N. M. Nuzaihan, and C. H. Voon, *Anal. Chim. Acta* 917, 1 (**2016**).
8. M. N. M. Nuzaihan, U. Hashim, A. R. Ruslinda, M. K. Md Arshad, and M. H. A. Baharin, *Curr. Nanosci.* 11, 239 (**2015**).
9. S. Kim, J. Kim, J. Jang, H.-S. Mo, D. M. Kim, S.-J. Choi, B.-G. Park, D. H. Kim, and J. Park, *J. Nanosci. Nanotechnol.* 17, 3257 (**2017**).
10. Y. Hong, W.-M. Kang, I.-T. Cho, J. Shin, M. Wu, and J.-H. Lee, *J. Nanosci. Nanotechnol.* 17, 3151 (**2017**).
11. J. Jang, J. Kim, S. Kim, H.-S. Mo, D. M. Kim, S.-J. Choi, B.-G. Park, D. H. Kim, and J. Park, *J. Nanosci. Nanotechnol.* 17, 3146 (**2017**).
12. X. Han, S. Li, Z. Peng, A. M. Othman, and R. Leblanc, *ACS Sensors* 1, 106 (**2016**).
13. M. Kaisti, Z. Boeva, J. Koskinen, S. Nieminen, and K. Levon, *ACS Sensors* 1, 1423 (**2016**).
14. S.-M. Koo, Q. Li, M. D. Edelstein, C. A. Richter, and E. M. Vogel, *Nano Lett.* 5, 2519 (**2005**).
15. I.-K. Lee, T.-E. Bae, H.-C. Lau, J.-O. Lim, and W.-J. Cho, *Sens. Lett.* 12, 1003 (**2014**).
16. W. Tang, L. Li, and X. Zeng, *Talanta* 131, 417 (**2015**).
17. P. Kar, A. Pandey, J. J. Greer, and K. Shankar, *Lab Chip* 12, 821 (**2012**).
18. A. N. Banerjee, *Nanotechnol. Sci. Appl.* 4, 35 (**2011**).
19. H. Lee, M. Y. Song, J. Jurng, and Y.-K. Park, *Powder Technol.* 214, 64 (**2011**).
20. M. F. M. Fathil, M. K. Md Arshad, S. C. B. Gopinath, U. Hashim, R. Adzhri, R. M. Ayub, A. R. Ruslinda, M. N. M. Nuzaihan, A. H. Azman, M. Zaki, and T. H. Tang, *Biosens. Bioelectron.* 70, 209 (**2015**).
21. B. Rezaei, M. Ghani, A. M. Shoushtari, and M. Rabiee, *Biosens. Bioelectron.* 78, 513 (**2016**).
22. C. L. Cowles and X. Zhu, *Biosens. Bioelectron.* 30, 342 (**2011**).
23. W. Shen, D. Tian, H. Cui, D. Yang, and Z. Bian, *Biosens. Bioelectron.* 27, 18 (**2011**).
24. R. F. Dutra and L. T. Kubota, *Clin. Chim. Acta* 376, 114 (**2007**).
25. B. Zhang, A. W. Morales, R. Peterson, L. Tang, and J. Y. Ye, *Biosens. Bioelectron.* 58, 107 (**2014**).
26. V. Palamalai, M. M. Murakami, and F. S. Apple, *Clin. Biochem.* 46, 1631 (**2013**).
27. T. S. Senthil, N. Muthukumarasamy, S. Agilan, M. Thambidurai, and R. Balasundaraprabhu, *Mater. Sci. Eng. B* 174, 102 (**2010**).
28. F. P. Gökdemir, E. Yüzbaşıoğlu, B. Keskin, O. Özdemir, and K. Kutlu, *Advanced Materials Letter* 5, 367 (**2014**).
29. Q. Yu, M.-M. Mao, Q.-J. Li, X.-Q. Fu, H. Tian, J.-X. Li, S. X. Mao, and Z. Zhang, *Nano Lett.* 16, 1156 (**2016**).
30. A. K. M. Muaz, U. Hashim, F. Ibrahim, K. L. Thong, M. S. Mohktar, and W. W. Liu, *Microsyst. Technol.* 22, 871 (**2015**).
31. K.-R. Choi, J.-C. Woo, Y.-H. Joo, Y.-S. Chun, and C.-I. Kim, *Vacuum* 92, 85 (**2013**).
32. M. R. Kupsta, M. T. Taschuk, M. J. Brett, and J. C. Sit, *IEEE Sensors Journal* 9, 1979 (**2009**).
33. M. K. Md Arshad, N. Othman, and U. Hashim, *Crit. Rev. Solid State Mater. Sci.* 40, 182 (**2015**).
34. G. Korotcenkov, I. Boris, V. Brinzari, S. H. Han, and B. K. Cho, *Sensors Actuators B Chem.* 182, 112 (**2013**).
35. M. Menetrey, A. Markovits, and C. Minot, *Surf. Sci.* 524, 49 (**2003**).
36. S. Wang, L. Pan, J. J. Song, W. Mi, J. J. Zou, L. Wang, and X. Zhang, *J. Am. Chem. Soc.* 137, 2975 (**2015**).
37. J. Nowotny, M. A. Alim, T. Bak, M. A. Idris, M. Ionescu, K. Prince, M. Z. Sahdan, K. Sopian, M. Asri, M. Teridi, and W. Sigmund, *Chem. Soc. Rev.* 44, 8424 (**2015**).
38. J. Nowotny, M. A. Alim, T. Bak, M. A. Idris, M. Ionescu, K. Prince, M. Z. Sahdan, K. Sopian, M. A. Mat Teridi, and W. Sigmund, *Chem. Soc. Rev.* 44, 8424 (**2015**).
39. B. Wang, R. Jing, H. Qi, Q. Gao, and C. Zhang, *J. Electroanal. Chem.* 781, 212 (**2016**).
40. T. Kong, R. Su, B. Zhang, Q. Zhang, and G. Cheng, *Biosens. Bioelectron.* 34, 267 (**2012**).
41. A. B. Mattos, T. A. Freitas, L. T. Kubota, and R. F. Dutra, *Biochem. Eng. J.* 71, 97 (**2013**).
42. A. Periyakaruppan, R. P. Gandhiraman, M. Meyyappan, and J. E. Koehne, *Analytical Chemistry* 85, 3858 (**2013**).
43. S. M. Seo, S. W. Kim, J. N. Park, J. H. Cho, H. S. Kim, and S. H. Paek, *Biosens. Bioelectron.* 83, 19 (**2016**).
44. A. Sharma, C. H. Han, and J. Jang, *Biosens. Bioelectron.* 82, 78 (**2016**).

IP: 185.14.195.115 On: Tue, 2[illegible] Copyright: American Scientific Publishers Delivered by [illegible]

Received: 20 April 2017. Accepted: 27 May 2017.